^{176}Lu: An unreliable *s*-process chronometer

K. T. Lesko, E. B. Norman, R-M. Larimer, and B. Sur
Nuclear Science Division, Lawrence Berkeley Laboratory, 1 Cyclotron Road, Berkeley, California 94720 and Center for Particle Astrophysics, University of California, Berkeley, California 94720

C. B. Beausang*
Nuclear Science Division, Lawrence Berkeley Laboratory, 1 Cyclotron Road, Berkeley, California 94720
(Received 17 October 1990)

A level scheme of ^{176}Lu up to ~1400 keV excitation energy is deduced from a γ-γ coincidence experiment and previously published particle transfer data. 170 γ-ray transitions are placed between 85 levels. We identify 27 previously unknown levels and 131 previously unknown transitions in ^{176}Lu. With this γ-ray data we place the energy of the isomer at 122.9 keV. A level at 838.5 keV ($J^\pi=5^-$, $t_{1/2}<10$ ns) is found to decay with substantial strength to both the ground state (7^-, 4.08×10^{10} yr) and the 122.9 keV isomer (1^-, 3.7 hr). The presence of this level guarantees the thermal equilibrium of ^{176}Lu^{g,m} for $T\geq3\times10^8$ K and therefore during *s*-process nucleosynthesis. The resulting temperature sensitivity of its effective half-life rules out the use of ^{176}Lu as an *s*-process chronometer. The use of ^{176}Lu to determine *s*-process temperatures is discussed.

INTRODUCTION

^{176}Lu is one of the few naturally occurring radio nuclides that have survived from the era of nucleosynthesis. Its present isotopic abundance [1] is 2.6% and its half-life is 4.08×10^{10} yr [2]. The spectrum of gamma rays from the ground-state decay of ^{176}Lu nuclei in a foil of natural lutetium observed by a 1.3-cm-thick planar germanium detector is shown in Fig. 1.

As shown in Fig. 2, ^{176}Lu can be produced only via the slow neutron capture process (*s* process). The stable isobars ^{176}Yb and ^{176}Hf shield this nucleus from rapid neutron capture and proton capture contributions. The *s*-process production path in the vicinity of ^{176}Lu is also indicated in the figure. Due to the long half-life of the ground state, ^{176}Lu^g, it was suggested that ^{176}Lu would be a candidate for an *s*-process chronometer [3,4]. However, there exists a much shorter lived isomer at 122.9 keV ($J^\pi=1^-, t_{1/2}=3.7$ hr) [1]. As Fig. 3 shows, the large spin difference between these two levels prevents decays from the isomer to the ground state; rather the isomer β decays to ^{176}Hf. The presence of this isomer could affect the decay of ^{176}Lu in astrophysical environments, providing a method of communication exists between the two levels. An example of this communication is illustrated in Fig. 3 where an additional level of intermediate spin is populated and subsequently decays to both the ground state and the isomer. The time scale for obtaining equilibration between the isomer and g.s. is determined by the rate of excitation of the mediating level, its spin, parity, and excitation energy, and its decay properties, as well as the half-lives of the g.s. and isomer. In the stellar environment where the *s* process occurs, nuclei are believed to be subjected to temperatures of the order of a few $\times10^8$ K. At these temperatures one can expect that the tails of the thermal distribution should populate levels up to ~1 MeV.

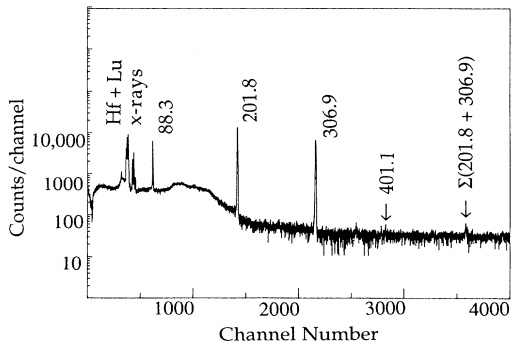

FIG. 1. The ^{176}Lu^g decay spectrum observed from a sample of ^{nat}Lu. The principal peaks from ^{176}Lu are labeled by their energy in units of keV.

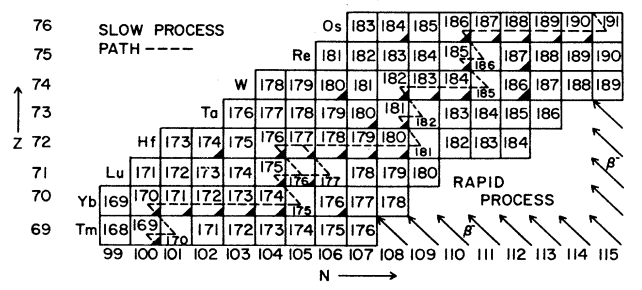

FIG. 2. The *s*-process path in the vicinity of ^{176}Lu. The stability of ^{176}Yb and ^{176}Hf guarantees that ^{176}Lu can only be produced in the *s* process.

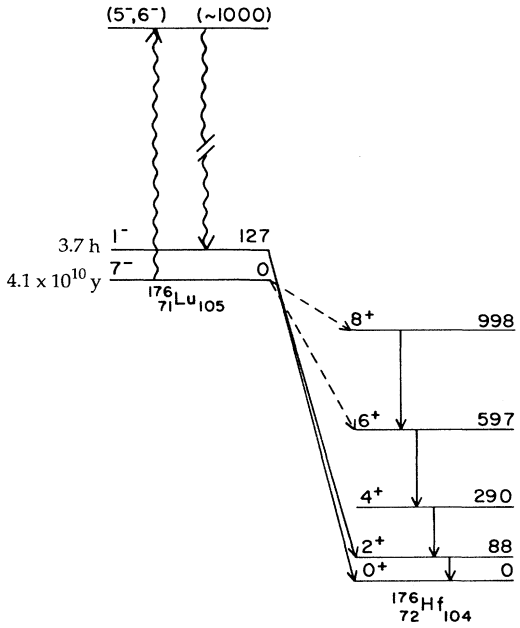

FIG. 3. A partial level scheme of ^{176}Lu, showing the positions and decays of the ground state and isomer at 122.9 keV. The equilibration of these two levels could be achieved by way of a level of intermediate spin, as illustrated in the figure.

The presence of such an equilibration path would severely compromise the usefulness of ^{176}Lu as an *s*-process chronometer due to the effective decay constant λ_{eff} being temperature sensitive. Such a mediating level lying between 662 and 1332 keV excitation energy can be inferred from the photoexcitation work of Norman *et al.* [5]. In these experiments, ^{176}Lu^{m} activity was observed following the irradiation of a $^{\text{nat}}$Lu foil with ^{60}Co γ rays, but not following irradiation with a ^{137}Cs source. Our aim in this experiment was, therefore, to determine the level scheme of ^{176}Lu up to approximately 1 MeV to search for levels which could serve as a mediating level between the ground state and isomer. We pursued this goal using the method of coincident gamma-ray detection. In analyzing this experiment we obtained a comprehensive understanding of the levels and transitions in ^{176}Lu, which we report here in addition to our astrophysical conclusions. Concurrently and independently another group pursued a different technique to establish the level scheme, obtaining similar results and identical conclusions [6,7].

EXPERIMENT

We used the ^{176}Yb$(p,n)^{176}$Lu reaction to populate levels in ^{176}Lu. An 8-MeV proton beam was provided by Lawrence Berkeley Laboratory's 88-Inch Cyclotron. The beam energy was chosen to maximize the yield of ^{176}Lu while limiting other reaction products. The target was a 2 mg/cm^2 metallic foil enriched to 97.04% ^{176}Yb. Data collection was count-rate limited and required that beam currents were kept below 10 nA. Coincident gamma-ray and gamma-ray singles events were detected by the High Energy Resolution Array of 21 Compton-suppressed germanium detectors. The detector at zero degrees to the beam was removed to install a shielded external beam dump for the unscattered protons. Approximately 60×10^6 coincident events were recorded. These events were then sorted off-line into a two-dimensional matrix. Detector resolution was found to be 2.32 keV FWHM at 838.5 keV, with no significant decrease in resolution in the sum spectrum as compared to that of a single detector. Detector energy and efficiency calibrations were performed with standard sources placed at the target position. In addition to the energy signals, we generated timing information signals (TAC) between detectors. A subset of ten of the detectors were designated as start detectors and the stop signal was generated by a coincident event in any of the other ten detectors. The hardware gate of 100 ns established the maximum time difference between coincident events. The resolution of the TAC was $\sim$10 ns.

ANALYSIS AND RESULTS

Gates were placed on $\sim$400 of the strongest transitions and coincidence relationships were established in the background subtracted gated spectra. Using these data, the previously established level scheme, and ^{176}Lu levels established with particle transfer experiments, we constructed the level scheme shown in Figs. 4–10. In these figures, the levels and decay transitions have been grouped into band structures. These groupings are supported by data in the literature and by the work of Refs. [6] and [7]. Those levels and transitions that did not fit into known bands are presented in Figs. 8 and 9. In all, we have proposed 170 transitions between 85 levels. We have emphasized the transitions that feed and decay from the 838.5 keV level in Figure 10. In Table I we present our proposed transitions and levels in ^{176}Lu as well as those recently reported in a recent evaluation [8].

Many of these proposed placements confirm previous work. All proposed levels were checked for self-consistency with parallel and sequential decays and for γ-decay intensities. The relative intensities of all transitions from each level were confirmed to be independent of which populating transition was gated on. No attempt was made to determine the spins and parities of the transitions from the intrinsic angular distribution data, rather data from the literature [4,6–16] were used to assign the spins and parities suggested in Figs. 4–10. In a few cases we report levels which have not been previously observed, we propose a range of spins based upon the properties of the subsequent levels, typically assuming that

transitions which change the spin by two units would be fast enough to be observed in our experiment. In Table II we present the level energies, spins, and parities of our deduced levels as well as those of Klay [7] and the recent evaluations [8].

As can be seen in Fig. 10, where we have highlighted the transitions from and to the level at 838.5 keV, this level decays with significant decay strengths to both the ground state and to the isomer. We present in Fig. 11, the spectrum of γ rays gated on the 208 and 402 keV transitions to the 838.5 keV level. Decays placed to the ground state and the isomer are indicated by arrows in the figure. From the transitions shown in the Fig. 10 we can infer the (J,π) of this level as being 5 or 6. This inference is obtained by assuming that strongly observed transitions will have $\Delta J \leq 2\hbar$. The 838.5 keV level is observed

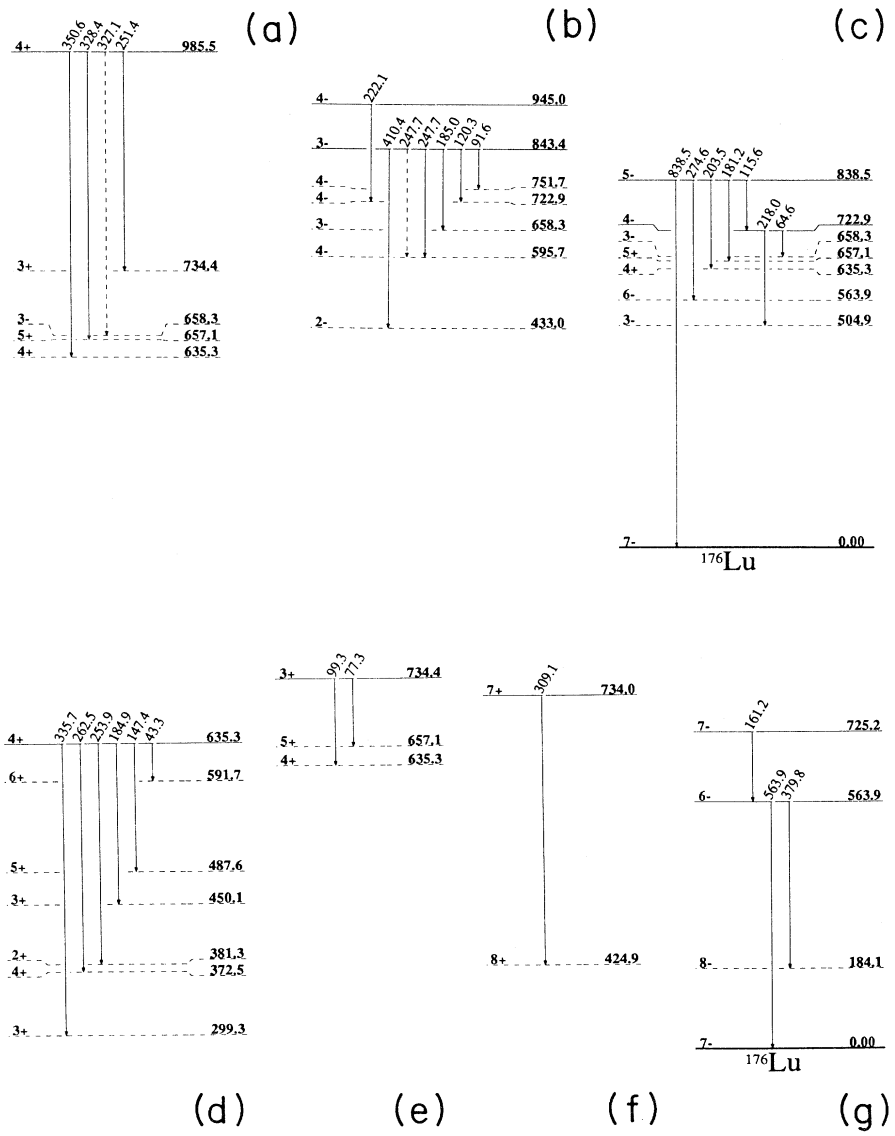

FIG. 4. The proposal level scheme of ^{176}Lu. We present the levels in band structures where possible, relying on earlier experiments to assign bandheads and members to specific bands. The decay energies and the level energies are given in keV. The spins and parities are obtained from the literature. In this and the following six figures, those levels which are contained within the decay band are shown with solid lines, whereas the decays to levels in other bands (also seen in this experiment) are shown with dashed lines. In (a) the band based upon $p\frac{1}{2}^{+}[411]-n\frac{9}{2}^{+}[624]$ is presented, (b) $p\frac{1}{2}^{+}[411]-n\frac{7}{2}^{-}[514]$, (c) $p\frac{1}{2}^{+}[411]+n\frac{7}{2}^{-}[514]$, (d) $p\frac{1}{2}^{-}[541]+n\frac{7}{2}^{-}[514]$, (e) $p\frac{1}{2}^{-}[541]-n\frac{7}{2}^{-}[514]$, (f) $p\frac{5}{2}^{+}[402]+n\frac{9}{2}^{+}[624]$, and (g) $p\frac{5}{2}^{+}[402]+n\frac{7}{2}^{-}[514]$.

to decay to levels with spins $=4^-$, 4^+, 5^+, 6^-, 7^-. This range of assignments agrees with the assignment of 5^- suggested in the literature and with the assignment deduced in Refs. [6] and [7]. We, therefore, adopt the value of 5^- as proposed by the comprehensive neutron capture work of Klay [6,7] for this previously unspecified level. For the specific transitions originating from this level we have measured the decay strengths, corrected for detector efficiency, but not for internal conversion. These are presented in Table III. The errors are estimates of only the statistical errors involved in extracting the peak areas. In addition, to corroborate the decays to and from the level at 838.5 keV, we generated the TAC spectra for all combinations of start detectors feeding and stop detectors decaying from this level. These TAC spectra all showed the same time relationships between all combinations of the feeding and exiting γ rays which increases our confidence in their placement.

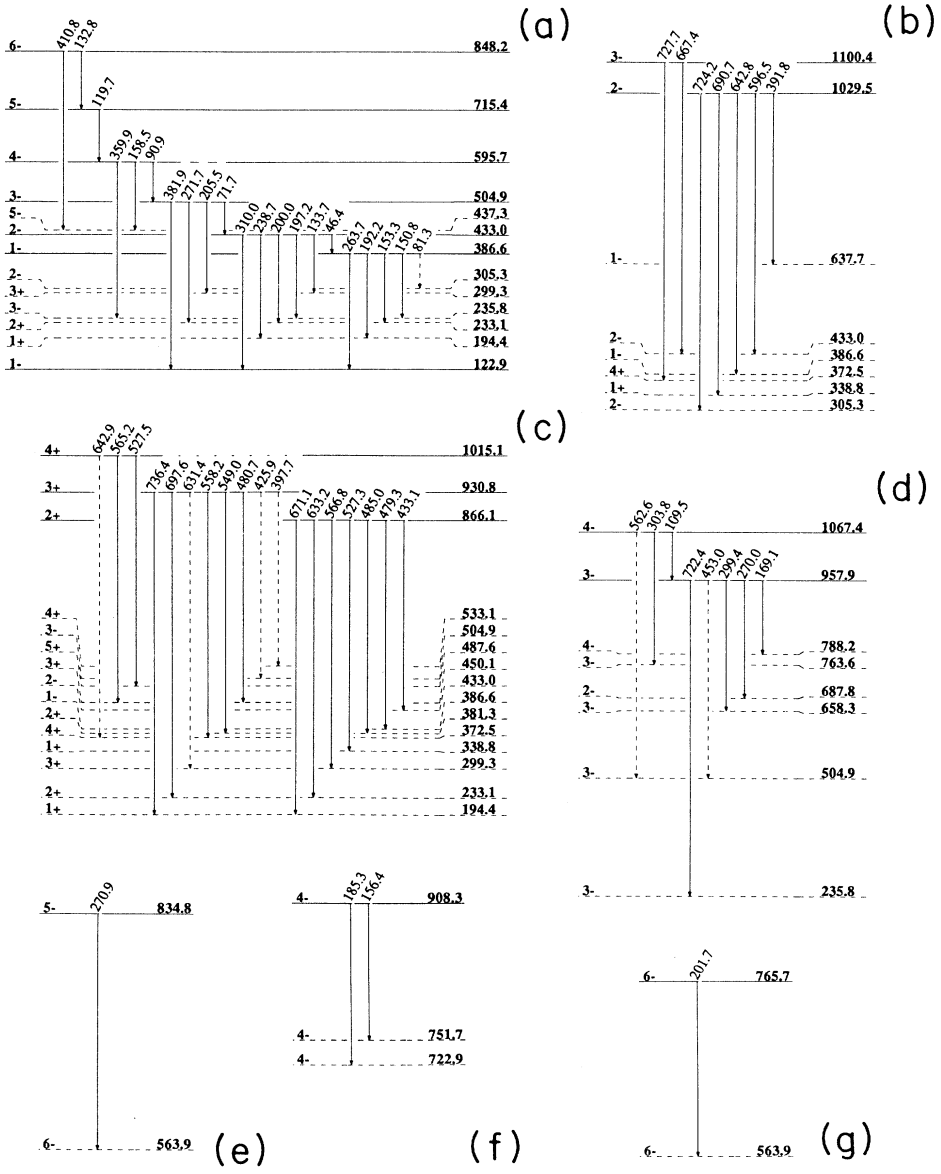

FIG. 5. Additional band structures for ^{176}Lu. In (a) the band based on $p\frac{5}{2}^+[402]-n\frac{7}{2}^-[514]$ is presented, (b) $p\frac{7}{2}^+[404]-n\frac{3}{2}^-[512]$, (c) $p\frac{5}{2}^+[402]-n\frac{9}{2}^+[624]$, (d) $p\frac{7}{2}^+[404]-n\frac{1}{2}^-[521]$, (e) $p\frac{7}{2}^+[404]+n\frac{3}{2}^-[512]$, (f) $p\frac{7}{2}^+[404]+n\frac{1}{2}^-[521]$, and (g) $p\frac{7}{2}^+[404]+n\frac{5}{2}^-[512]$.

From the placement of this level and its inferred spin we can calculate the photoexcitation rate as a function of temperature using the expression [17]

$$\frac{\tau(I \Longrightarrow I^*)}{\tau_{\rm sp}(I^* \Longrightarrow I)} = \frac{(2J_I+1)}{(2J_{I^*}+1)} \left[\exp\left[\frac{\Delta E}{kT} \right] - 1 \right] . \qquad (1)$$

$\tau_{\rm sp}$ is the spontaneous decay rate, J_I and J_{I^*} are the spins of the states I and I^*, and ΔE is the energy difference between these two states. From our TAC data we could place an upper limit on the spontaneous decay lifetimes of the potentially mediating levels of $\tau_{\rm sp} \leq 10$ ns, which is consistent with the observed resolution. The single-particle Weisskopf estimates for the rates of these decays are substantially faster than this limit. Using the theoretical estimates for $\tau_{\rm sp}$ we present the three curves in Fig. 12 corresponding to the population of the 838.5, 722.9, and 563.9 keV levels from the ground state. Assuming that the photoexcitation times is short in comparison to the meanlife of the isomer establishes the criterion for thermal equilibrium. We see in Fig. 12 that for temperatures greater than 3×10^8 K, the isomer and ground state will be in thermal equilibrium using the 838.5 keV level as the mediating level. From Fig. 4, we might also expect that the bandhead at 722.9 keV would serve as a mediating level. Calculating the single-particle transition

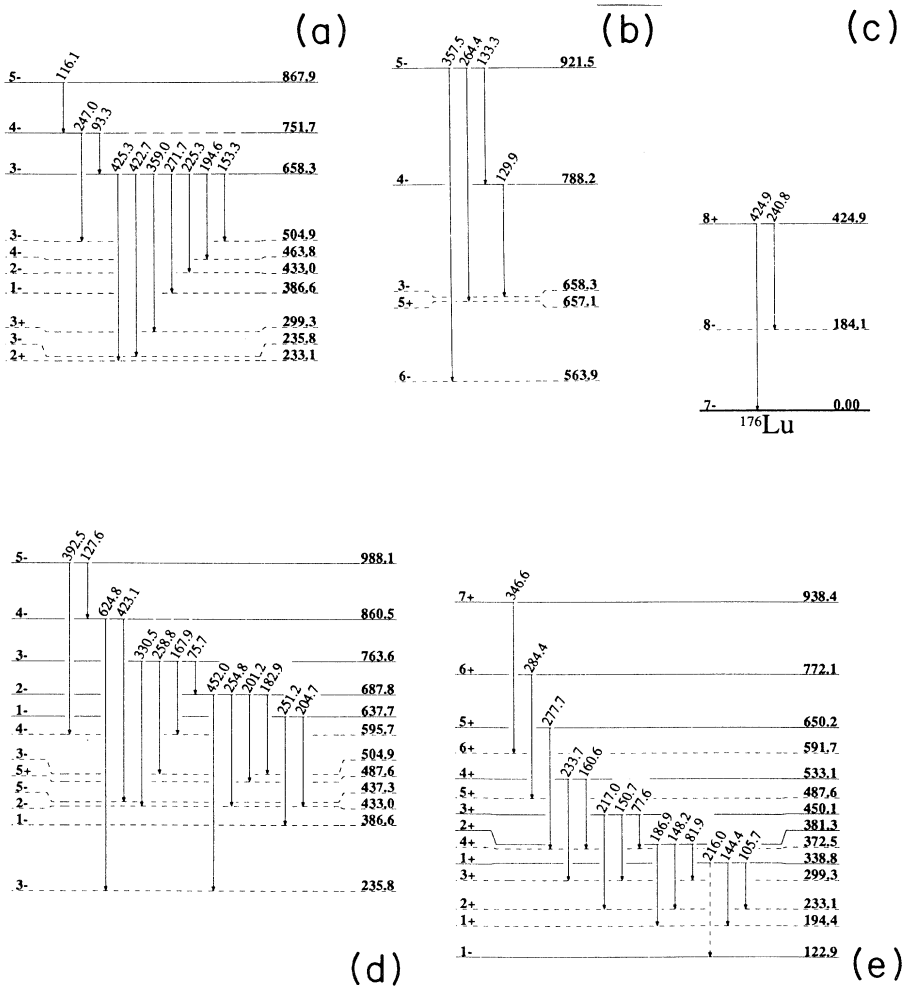

FIG. 6. Additional band structures for ^{176}Lu. In (a) the band based on $p\frac{7}{2}^+[404]-n\frac{1}{2}^-[510]$ is presented, (b) $p\frac{7}{2}^+[404]+n\frac{1}{2}^-[510]$, (c) $p\frac{7}{2}^+[404]+n\frac{9}{2}^+[624]$, $p\frac{7}{2}^+[404]-n\frac{5}{2}^-[512]$, and (e) $p\frac{7}{2}^+[404]-n\frac{9}{2}^+[624]$.

strength for this level we find that the direct decay from the 722.9 to the ground state would be only ~3% of the 838.5 decay strength. Consequently, it is possible that we would not directly observe this decay with our coincident gamma-ray technique. However, even a 1% branch to the ground state would be adequate to equilibrate the ground state and isomer via this level. Evaluating Eq. (1), assuming the moderating level is at 722.9 keV rather than 838.5 keV, yields an estimate of the equilibration temperature of 2.6×10^8 K. A more careful examination of the level scheme yields several other levels that could act as mediating levels, the lowest one being at 563.9 keV. This level results in equilibration being reached at 2×10^8 K.

The resulting effective half-life of ^{176}Lu is an extremely sensitive function of the temperature. The effective beta-decay rate, λ_{eff}, for the nucleus is given by

$$\lambda_{\text{eff}}=\frac{\sum_i g_i\lambda_i \exp(-E_i/kT)}{\sum_i g_i \exp(-E_i/kT)}\ , \tag{2}$$

where $g_i=(2J_i+1)$, λ_i is the beta-decay rate of the state i, E_i is the excitation energy of state i, and the summation is extended over all states that are in thermal equilibrium. Assuming that none of the other states are involved besides the ground state and the isomer (we would not expect any of the other levels to have drastically larger β-decay rates) this expression simplifies to

$$\lambda_{\text{eff}}(^{176}\text{Lu})=\frac{2.54\times10^{-10}+4.93\times10^3\exp(-14.26/T_8)}{15+3\exp(-14.26/T_8)}(\text{y}^{-1})\ , \tag{3}$$

where T_8 is the temperature in units of 10^8 K. We have tabulated the solutions of this equation for the temperature range $0<T_8<5$ in Table IV. We compare our estimates to those of Refs. [18] and [19] which differ from ours in several respects. Cosner and Truran [18] assumed that all levels up to 300 keV contribute to the decay rate. However, Cosner and Truran and Takahashi and Yokoi [19] both used an incorrect value for the isomer energy

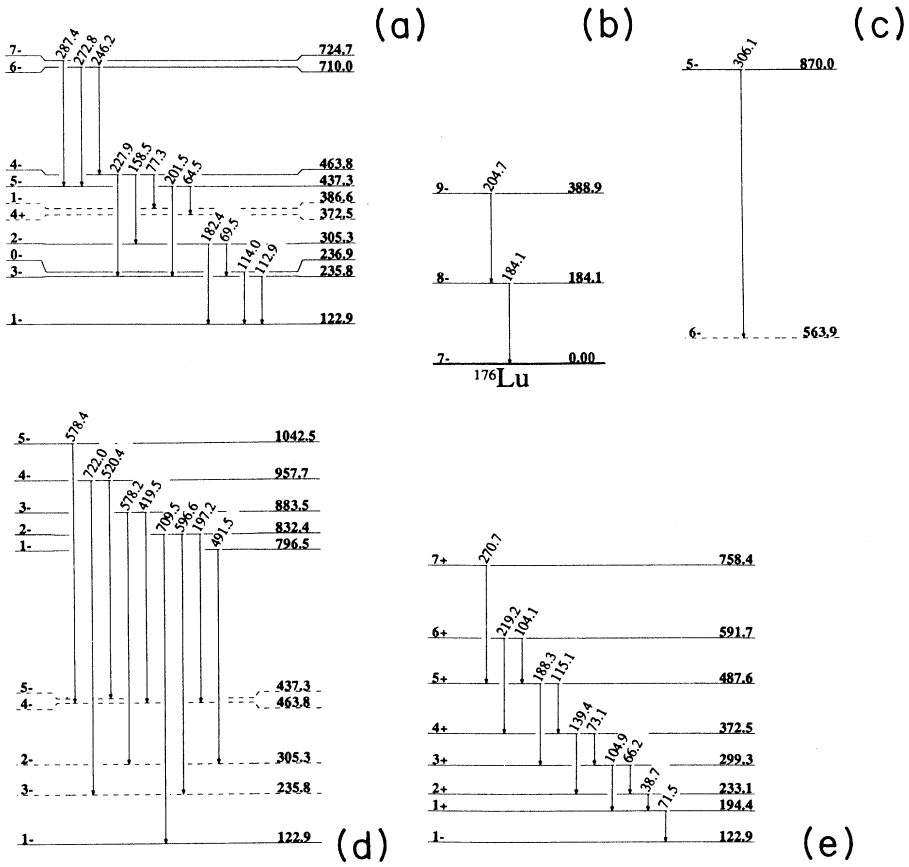

FIG. 7. Additional band structures for ^{176}Lu. In (a) the band based on $p\frac{7}{2}^+[404]-n\frac{7}{2}^-[514]$ is presented, (b) $p\frac{7}{2}^+[404]+n\frac{7}{2}^-[514]$, (c) is a gamma-vibrational band, (d) $p\frac{9}{2}^-[514]-n\frac{9}{2}^+[624]$, and (e) $p\frac{9}{2}^-[514]-n\frac{7}{2}^-[514]$.

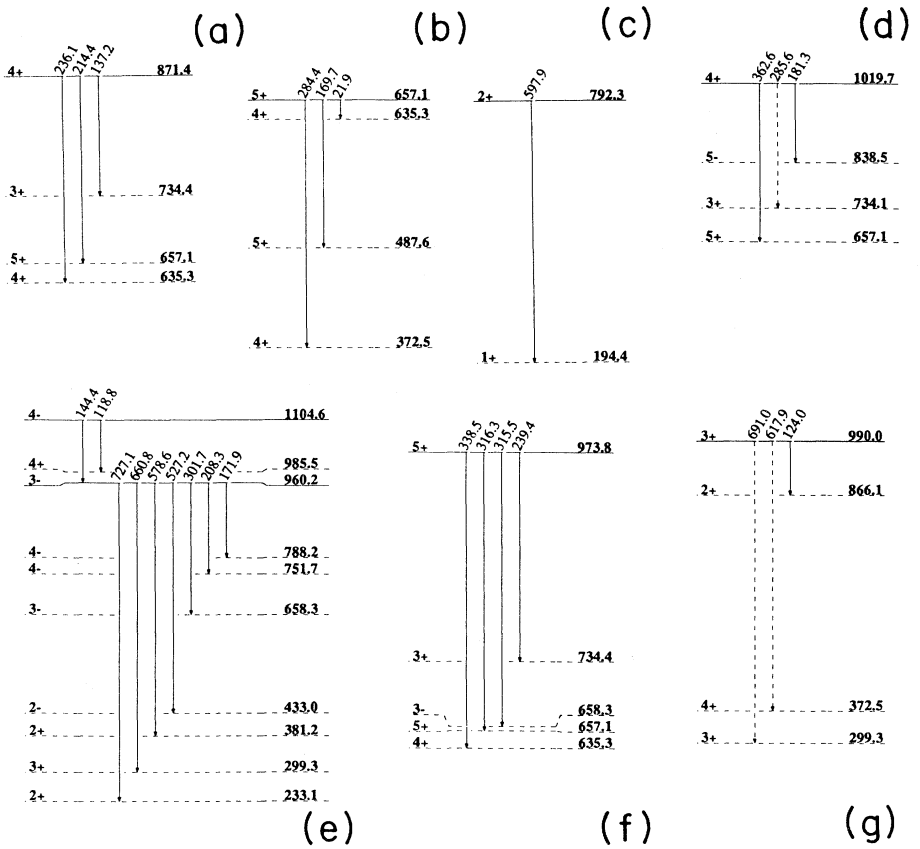

FIG. 8. Additional band structure for ^{176}Lu. In (a) the band based on $p\frac{9}{2}^{-}[514]-n\frac{1}{2}^{-}[510]$ is presented, (b) $p\frac{9}{2}^{-}[514]+n\frac{1}{2}^{-}[510]$. The decays presented in (c)–(g) are not assigned to bands. The spins and parities are taken from the literature.

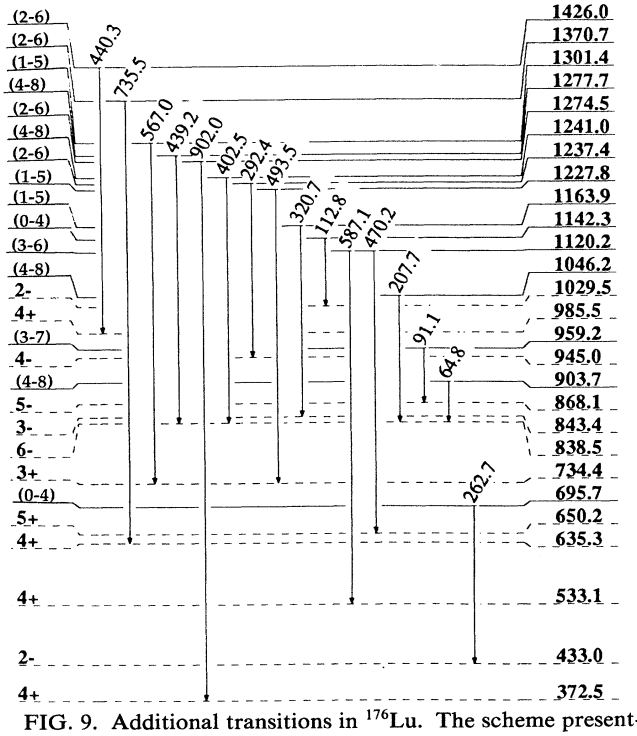

FIG. 9. Additional transitions in ^{176}Lu. The scheme presented has approximate values of spin based upon the decay properties of the levels.

which was in the literature (127 keV as opposed to the value we report of 122.9 keV). Table IV vividly illustrates how a relatively small change in the *s*-process temperature can result in a major change in the decay constant for ^{176}Lu. This strong temperature sensitivity quite effectively rules out ^{176}Lu for use as an cosmochronometer.

A second analysis of the $A=176$ system is based on the formalism of Schramm and Wasserberg [20]. In this analysis the mean duration of nucleosynthesis, $\Delta_{\max}$, can be expressed as

$$\Delta_{\max}=\frac{1}{\lambda_{^{176}\mathrm{Lu}}}\ln\left[\frac{B\langle N_s\sigma\rangle_{176}}{N_{^{176}\mathrm{Lu}}\langle\sigma_{^{176}\mathrm{Lu}}\rangle}\right], \quad (4)$$

where $\lambda_{^{176}\mathrm{Lu}}$ is the decay constant of ^{176}Lu, $\langle N_s\sigma\rangle_{176}$ is the product of the *s*-process abundance and the Maxwellian-averaged neutron capture cross section evaluated at mass 176 and at *s*-process temperatures ($T\sim 23$ keV). $N_{^{176}\mathrm{Lu}}$ is the present day abundance of ^{176}Lu, and $\langle\sigma_{^{176}\mathrm{Lu}}\rangle$ is the ~ 23 keV ^{176}Lu$(n,\gamma)^{177}$Lu cross section. Finally, B is the branching ratio for the formation of the ground state in the ^{175}Lu$(n,\gamma)^{176}$Lu reaction. The determination of B has been the subject of much experimental work in recent years [21–28], and the exact determina-

TABLE I. The γ-ray transitions identified in ^{176}Lu. The first three columns list the transition energy, the initial level, and the final level for the transitions. In the fourth and fifth columns we reproduce the transitions and initial levels reported in Ref. [8]. All energies are in keV. The ellipses indicate that a transition was not observed. Values in brackets are tentative assignments.

This work			Nucl. Data Sheets [8]		This work			Nucl. Data Sheets [8]	
E_{gamma}	E_{init}	E_{final}	E_{gamma}	E_{init}	E_{gamma}	E_{init}	E_{final}	E_{gamma}	E_{init}
21.9	657.1	635.3	...	...	148.2	381.3	233.1	148.218	381.475
38.7	233.1	194.4	38.745	233.256	150.7	450.1	299.3	150.752	450.246
43.3	635.3	591.7	...	...	150.8	386.6	235.8	...	...
46.4	433.0	386.6	46.453	433.159	...	...	...	151.69	533.188
64.5	437.3	372.5	...	...	153.3	386.6	233.1	153.456	386.707
64.6	722.9	658.3	64.462	723.022	153.3	658.3	504.9	...	...
64.8	903.7	838.5	...	...	...	...	...	156.31	752.006
66.2	299.3	233.1	66.226	299.485	156.4	908.3	751.7	...	...
69.5	305.3	235.8	69.500	305.415	158.5	463.8	305.3	158.49	463.902
71.5	194.4	122.9	71.510	194.511	158.5	595.7	437.3	...	...
71.7	504.9	433.0	71.832	504.989	160.6	533.1	372.5	160.63	533.188
73.1	372.5	299.3	73.134	372.620	161.2	725.2	563.9	...	...
75.7	763.6	687.8	75.758	763.716	...	...	...	162.70	595.849
77.3	463.8	386.6	...	...	...	...	...	162.70	1032
77.3	734.4	657.1	...	...	167.9	763.6	595.7	167.867	763.716
77.6	450.1	372.5	...	...	169.1	957.9	788.2	...	...
[81.3]	386.6	305.3	81.285	386.707	169.7	657.1	487.6	169.48	657.235
81.9	381.3	299.3	81.990	381.475	171.9	960.2	788.2	...	...
90.9	595.7	504.9	90.859	595.849	181.2	838.5	657.1	...	...
91.1	959.2	867.9	...	...	181.3	1019.7	838.5	...	...
91.6	843.4	751.7	...	...	...	...	...	181.496	773.369
93.3	751.7	658.3	93.444	752.006	182.4	305.3	122.9	182.406	305.415
...	...	...	96.902	860.624	182.9	687.8	504.9	182.97	687.973
99.3	734.4	635.3	...	...	184.1	184.1	0.0	184.114	184.114
104.1	591.7	487.6	104.12	591.242	184.9	635.3	450.1	185.015	635.289
104.9	299.3	194.4	104.975	299.485	185.0	843.4	658.3	...	...
105.7	338.8	233.1	105.728	338.982	185.3	908.3	722.9	...	...
...	...	...	109.51	945.3	186.9	381.3	194.4	186.975	381.475
109.5	1067.4	957.9	...	...	188.3	487.6	299.3	188.273	487.753
...	...	...	111.85	840	192.2	386.6	194.4	192.192	386.707
112.8	1142.3	1029.5	...	...	...	...	...	194.17	757
112.9	235.8	122.9	112.91	235.911	194.6	658.3	463.8	194.60	658.559
114.0	236.9	122.9	114.061	237.061	197.2	433.0	235.8	197.245	433.159
115.1	487.6	372.5	115.133	487.753	...	...	...	199.50	504.989
115.6	838.5	722.9	115.7	838.4	200.0	433.0	233.1	199.899	433.159
116.1	867.9	751.7	...	...	201.2	687.8	487.6	...	...
...	...	...	118.29	504.989	201.5	437.3	235.8	201.545	437.452
...	...	...	118.710	870.717	201.7	765.7	563.9	...	...
118.8	1104.6	985.5	...	...	...	...	...	203.394	1074
119.7	715.4	595.7	119.663	715.513	203.5	838.5	635.3	203.5	838.4
120.3	843.4	722.9	...	...	204.7	388.9	184.1	204.694	388.83
124.0	990.0	866.1	...	...	204.7	637.7	433.0	204.707	637.874
...	...	...	124.047	657.235	205.5	504.9	299.3	205.55	504.989
...	...	...	125.83	763.716	...	...	...	206.92	657.235
127.6	988.1	860.5	...	...	207.7	1046.2	838.5	...	...
...	...	...	129.759	1074	208.3	960.2	751.7	...	...
129.9	788.2	658.3	...	...	...	...	...	210.538	715.513
132.8	848.2	715.4	138.82	848.33	214.4	871.4	657.1	...	...
133.3	921.5	788.2	...	...	[216]	338.8	122.9	...	...
133.7	433.0	299.3	133.664	433.159	217.0	450.1	233.1	216.976	450.246
...	...	...	136.69	864	218.0	722.9	504.9	218.035	723.022
137.2	871.4	734.4	...	...	219.2	591.7	372.5	219.242	591.242
139.4	372.5	233.1	139.367	372.620	222.1	945.0	722.9	221.366	945.3
144.4	338.8	194.4	144.468	338.982	...	...	...	224.71	613.43
144.4	1104.6	960.2	...	...	225.3	658.3	433.0	225.389	658.559
...	...	...	145.135	860.624	227.9	463.8	235.8	227.988	463.902
147.4	635.3	487.6	147.538	635.289	233.7	533.1	299.3	233.722	533.188

TABLE I. (*Continued.*)

This work			Nucl. Data Sheets [8]		This work			Nucl. Data Sheets [8]	
E_{gamma}	E_{init}	E_{final}	E_{gamma}	E_{init}	E_{gamma}	E_{init}	E_{final}	E_{gamma}	E_{init}
236.1	871.4	635.3	...	...	359.9	595.7	235.8	359.94	595.849
238.7	433.0	194.4	238.656	433.159	362.6	1019.7	657.1	...	...
...	...	...	239.32	1074	368.6	832.4	463.8	...	...
239.4	973.8	734.4	...	...	379.8	563.9	184.1	387.4	565
...	...	...	240.21	773.369	381.9	504.9	122.9	381.8	504.989
240.8	424.9	184.1	...	...	...	...	...	388.843	388.83
246.2	710.0	463.8	246.2	710.19	391.8	1029.5	637.7	...	...
247.0	751.7	504.9	247.17	752.006	392.5	988.1	595.7	392.46	988.31
247.7	843.4	595.7	...	...	[397.7]	930.8	533.1	...	...
251.2	637.7	386.6	251.173	637.874	402.5	1241.0	838.5	...	...
251.4	985.5	734.4	...	...	410.7	843.4	433.0	...	...
...	...	...	252.47	848.33	410.8	848.2	437.3	...	...
253.9	635.3	381.3	253.857	635.289	419.5	883.5	463.8	...	...
254.8	687.8	433.0	254.817	687.973	422.7	658.3	235.8	422.69	658.559
258.8	763.6	504.9	258.77	763.716	423.1	860.5	437.3	...	...
262.5	635.3	372.5	262.658	635.289	424.9	424.9	0.0	...	...
262.7	695.7	433.0	...	...	425.3	658.3	233.1	425.40	658.559
263.7	386.6	122.9	263.727	386.707	[425.9]	930.8	504.9	...	...
264.4	921.5	657.1	...	...	...	...	...	429.24	613.43
...	...	...	264.708	860.624	433.1	866.1	433.0	...	...
270.0	957.9	687.8	...	...	439.2	1277.7	838.5	...	...
270.7	758.4	487.6	...	...	440.3	1426.0	985.5	...	...
270.9	834.8	563.9	...	...	...	...	...	446.3	752.006
271.7	504.9	233.1	...	...	452.0	687.8	235.8	...	...
271.7	658.3	386.6	271.839	658.559	[453]	957.9	504.9	...	...
...	...	...	272.7	988.31	470.2	1120.2	650.2	...	...
272.8	710.0	437.3	272.739	710.19	479.3	866.1	386.6	...	...
274.6	838.5	563.9	274.6	838.4	480.7	930.8	450.1	...	...
277.7	650.2	372.5	277.68	650.33	485.0	866.1	381.3	...	...
284.4	657.1	372.5	284.62	657.235	491.5	796.5	305.3	...	...
284.4	772.1	487.6	...	...	493.5	1227.8	734.4	...	...
[285.6]	1019.7	734.0	...	...	...	...	...	516.5	752.006
...	...	...	285.62	773.369	520.4	957.7	437.3	...	...
287.4	724.7	437.3	...	...	527.2	960.2	433.0	...	...
292.4	1237.4	945.0	...	...	527.3	866.1	338.8	...	...
...	...	...	296.22	595.849	...	...	...	527.47	1395.0
...	...	...	299.40	1032	527.5	1015.1	487.6	...	...
299.4	957.9	658.3	...	...	549.0	930.8	381.3	...	...
...	...	...	301.70	687.973	558.2	930.8	372.5	...	...
301.7	960.2	658.3	...	...	[526.6]	1067.4	504.9	...	...
303.8	1067.4	736.6	...	...	563.9	563.9	0.0	563.89	565
306.1	870.0	563.9	...	...	565.2	1015.1	450.1	...	...
309.1	734.4	424.9	...	...	566.8	866.1	299.3	...	...
310.0	433.0	122.9	310.16	433.159	567.0	1301.4	734.4	...	...
315.5	973.8	658.3	...	...	578.2	883.5	305.3	...	...
316.3	973.8	657.1	...	...	578.4	1042.5	463.8	...	...
320.7	1163.9	843.4	...	...	578.6	960.2	381.3	...	...
[327.1]	985.5	658.3	...	...	587.1	1120.2	533.1	...	...
328.4	985.5	657.1	...	...	596.5	1029.5	433.0	...	...
330.5	763.6	433.0	330.53	763.16	596.6	832.4	235.8	...	...
335.7	635.3	299.3	335.83	635.289	597.9	792.3	194.4	...	...
338.5	973.8	635.3	...	...	[617.9]	990.0	372.5	...	...
346.6	938.4	591.7	...	...	624.8	860.5	235.8	...	...
350.6	985.5	635.3	...	...	[631.4]	930.8	299.3	...	...
...	...	...	353.1	658.559	...	...	...	632.9	1395.0
355.7	860.5	504.9	355.65	860.624	633.2	866.1	233.1	...	...
...	...	...	357.5	657.235	642.8	1029.5	386.6	...	...
357.5	921.5	563.9	...	...	[642.9]	1015.1	372.5	...	...
359.0	658.3	299.3	359.0	658.559	660.8	960.2	299.3	...	...

TABLE I. (*Continued.*)

This work			Nucl. Data Sheets [8]	
E_{gamma}	E_{init}	E_{final}	E_{gamma}	E_{init}
667.4	1100.4	433.0	...	...
671.1	866.1	194.4	...	...
690.7	1029.5	338.8	...	...
[691]	990.0	299.3	...	...
697.6	930.8	233.1	...	...
709.5	832.4	122.9	...	...
722.0	957.7	235.8	...	...
722.4	957.9	235.8	...	...
724.2	1029.5	305.3	...	...
727.1	960.2	233.1	...	...
727.7	1100.4	372.5	...	...
735.5	1370.7	635.3	...	...
736.4	930.8	194.4	...	...
838.5	838.5	0.0	838.3	838.4
902.0	1274.5	372.5	...	...

tion of the isomer and ground-state capture cross sections critically affect the deduced parameter Δ_{max}. If we use the most recent values to evaluate the expression, presented in Table V, we find that the argument of the logarithm in Eq. (4) is less than unity, which results in a negative value for the mean age. This can be interpreted as implying that there exists more ^{176}Lu today than that estimated from the systematics of the *s* process. This excess of Lu could be explained by a readjustment of the isomer and ground-state fractions formed in the neutron capture reaction. By equilibrating the population, additional long-lived ground-state nuclei would be created, explaining the present-day "surplus" of ^{176}Lu.

The final topic we wish to address in this work is that of the use of ^{176}Lu as a stellar thermometer. In several other works [26,27] it has been suggested that if ^{176}Lu is in thermal equilibrium in stellar environments, then it would be possible to use the observed abundance of ^{176}Lu to deduce the stellar temperatures of the *s* process. How-

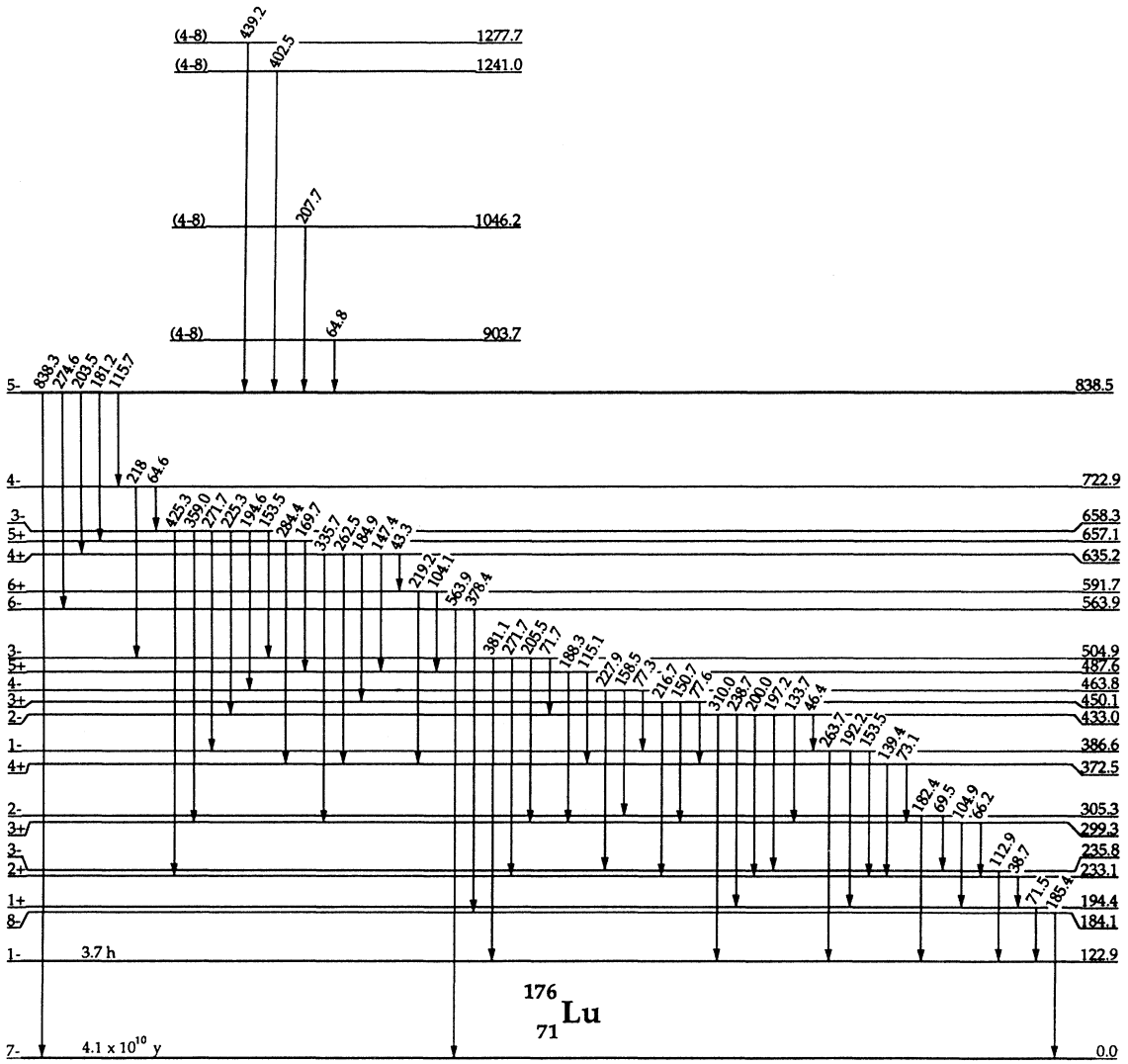

FIG. 10. A subset of the proposed level scheme emphasizing the transitions originating from and populating the level at 838.5 keV.

ever, to obtain the temperature profile during the *s* process will require a model-dependent analysis. Under the assumptions that the *s*-process neutron density and temperature are uniform, one can more easily extract limits on the *s*-process temperature. Klay *et al.* [6,7] have done this and obtain results consistent with other determinations of the *s*-process temperature.

In conclusion, we have established the level scheme of ^{176}Lu and have placed 170 transitions between 85 levels. Of these, 27 levels and 131 transitions were previously unknown. We have defined the energy of the isomeric level to be 122.9 keV through the γ-ray decay scheme. We have confirmed much of the previously published level and decay scheme for ^{176}Lu. The inferred spins for these levels are in agreement with a recent analysis by Klay [6,7] and we adopt the spins and parities for our lev-

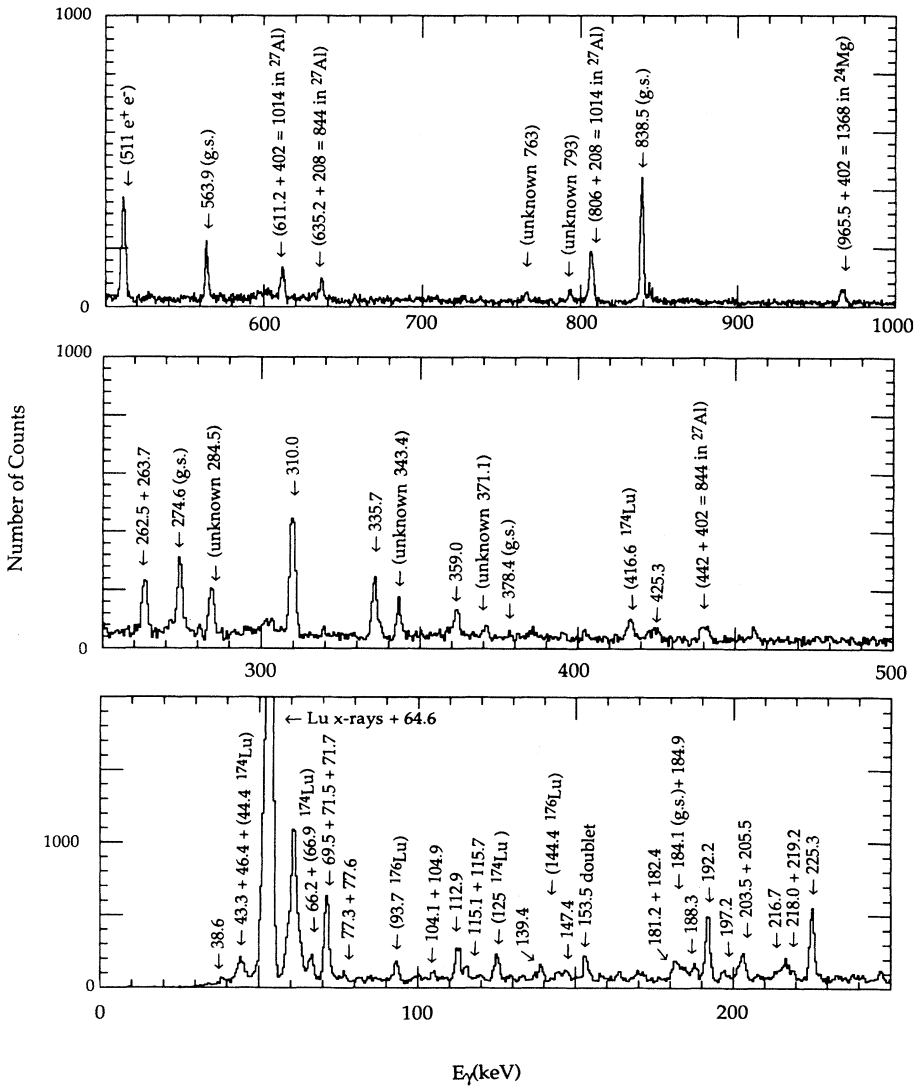

FIG. 11. The sum of two spectra of gamma rays from the 838.5 keV level gated by either the 402.5 or 207.7 keV transitions. Prominent decays to the isomer of ^{176}Lu have been identified by their transition energies (in keV). Decays to the ground state are additionally labeled with "g.s." Decays to other bands in ^{176}Lu or in other nuclei are presented in parentheses. A few unplaced gamma rays are labeled "unknown."

TABLE II. Comparison of the level energies, spins, and parities. We list the energies, spins, and parities for our deduced levels as well as those reported in the Ref. [7] and those presented in the recent evaluation [8]. All energies are in keV. The ellipses indicate that a level was not observed or placed by the quoted reference. Values in parentheses are tentative assignments.

This work		(*n*,gamma)		Nuclear Data Sheets	
Energy (±0.1)	Adopted J^π	Energy [7] (±0.01)	J^π	Energy [8]	J^π
0.0	7−	0.000	7−	0	7−
122.9	1−	122.855	1−	123(14)	1−
184.1	8−	184.130	8−	184.123(12)	(8)−
194.4	1+	194.372	1+	194.511(6)	(1)+
233.1	2+	233.117	2+	233.256(7)	(2)+
235.8	3−	235.776	3−	235.911(7)	(3)−
236.9	0−	236.925	0−	237.061(12)	(0−)
299.3	3+	299.357	3+	299.485(8)	(3)+
305.3	2−	305.277	2−	305.415(9)	(2)−
...	...	...	...	312(3)	...
338.8	1+	338.857	1+	338.982(10)	(1+)
372.5	4+	372.500	4+	372.620(0)	(4+)
381.3	2+	381.358	2+	381.475(11)	(2+)
386.6	1−	386.584	1−	386.707(8)	(1)−
388.9	9−	388.901	9−	388.83(2)	(9)−
...	...	...	...	400(2)	...
424.9	8+	424.891	8+	...	...
433.0	2−	433.042	2−	433.159(8)	(2)−
437.3	5−	437.344	5−	437.452(21)	(5)−
450.1	3+	450.120	3+	450.246(12)	(3)+
463.8	4−	463.344	4−	463.902(20)	(4)−
487.6	5+	487.645	5+	487.753(11)	(5)+
...	...	487.838	8+	486(3)	(8)+
504.9	3−	504.885	3−	504.989(10)	(3−)
533.1	4+	533.097	4+	533.188(15)	(4)+
563.9	6−	563.938	6−	565(3)	(6)−
...	...	...	...	∼578	...
591.7	6+	591.782	6+	591.870(17)	(6+)
595.7	4−	595.753	4−	595.849(112)	(4)−
...	...	613.430	10−	613.43(8)	(10−)
...	...	615.200	9+	...	...
...	...	...	...	623(3)	...
635.3	4+	635.207	4+	635.289(13)	3+,4+
637.7	1−	637.789	1−	637.874(16)	(1)−
650.2	5+	650.183	5+	650.30(3)	(5+)
657.1	5+	657.142	5+	657.235(17)	(5+)
658.3	3−	658.445	3−	658.559(14)	(3)−
687.8	2−	687.867	2−	687.973(23)	(2−)
...	...	693.804	5+	683(3)	(9)+
695.7	(0−4)	...	...	...	...
...	...	709.225	7+	...	...
710.0	6−	710.074	6−	710.19(3)	(6−)
715.4	5−	715.431	5−	715.513(15)	(5)−
722.9	4−	722.921	4−	723.022(15)	(4)−
724.7	7−	724.708	7−	...	...
725.2	7−	725.215	7−	...	...
734.0	7+	734.033	7+	...	...
734.4	3+	734.369	3+	734.0(3)	3+,4+
751.7	4−	751.893	4−	752.006(17)	(4−)
758.4	7+	758.403	7+	757(4)	(7)−
763.6	3−	763.635	3−	763.716(16)	(3−)
765.7	6−	765.681	6−	...	...
772.1	6+	772.063	6+	773.369(24)	(6+)
...	...	780.188	0−	...	...
...	...	786.266	4+	787.2(4)	...

TABLE II. (*Continued*).

This work		(*n*,gamma)		Nuclear Data Sheets	
Energy (±0.1)	Adopted J^π	Energy [7] (±0.01)	J^π	Energy [8]	J^π
788.2	4−	788.219	4−	· · ·	· · ·
792.3	2+	792.272	2+	· · ·	· · ·
796.5	1−	796.641	1−	· · ·	· · ·
· · ·	· · ·	· · ·	· · ·	814(1)	· · ·
· · ·	· · ·	826.400	10+	· · ·	· · ·
832.4	2−	832.410	2−	833.9(3)	3,4
834.8	5−	834.809	5−	· · ·	· · ·
838.5	5−	838.640	5−	838.4(3)	· · ·
· · ·	· · ·	· · ·	· · ·	840(2)	(3)−
843.4	3−	843.422	3−	843.2(4)	3,4
848.2	6−	848.246	6−	848.33(5)	(6−)
· · ·	· · ·	851.236	5+	· · ·	· · ·
· · ·	· · ·	854.667	7+	· · ·	· · ·
860.5	4−	860.564	4−	860.624(19)	(4−)
866.1	2+	866.364	· · ·	· · ·	· · ·
867.9	5−	868.099	5−	864(6)	(5)−
870.0	5−	870.003	5−	870.717(21)	(5−)
871.4	4+	871.275	4+	· · ·	· · ·
883.5	3−	883.474	3−	883.7(5)	3−,4−
903.7	(4–8)	· · ·	· · ·	903.5(3)	· · ·
908.3	4−	908.252	4−	907.3(6)	· · ·
· · ·	· · ·	909.637	2−	· · ·	· · ·
921.5	5−	921.472	5−	922.3(3)	2−,5−
930.8	3+	930.761	3+	929.9(8)	5+,(2+)
938.4	7+	938.400	7+	· · ·	· · ·
· · ·	· · ·	941.076	7−	· · ·	· · ·
945.0	4−	945.027	4−	945.3(3)	(4)−
957.7	4−	957.748	4−	958.9(5)	3,4
957.9	3−	957.894	3−	· · ·	· · ·
959.2	(3–7)	· · ·	· · ·	· · ·	· · ·
960.2	3−	960.193	3−	· · ·	· · ·
· · ·	· · ·	962.847	6−	· · ·	· · ·
· · ·	· · ·	· · ·	· · ·	966(3)	· · ·
· · ·	· · ·	972.519	6−	· · ·	· · ·
973.8	5+	973.763	5+	973.7(4)	5+,(2+)
985.5	4+	985.569	4+	· · ·	· · ·
988.1	5−	988.167	5−	988.31(4)	(5−)
990.0	3+	990.426	3+	· · ·	· · ·
· · ·	· · ·	1002.763	6−	1006(3)	· · ·
1015.1	4+	1015.370	4+	· · ·	· · ·
1019.7	4+	1019.934	4+	1018.3(3)	3+,4+
· · ·	· · ·	· · ·	· · ·	1021(2)	· · ·
1029.5	2−	1029.695	2−	1031.4(3)	3−,4−
· · ·	· · ·	· · ·	· · ·	1032(4)	(6−)
1042.5	5−	1042.529	5−	1042.6(3)	· · ·
1046.2	(4–8)	· · ·	· · ·	· · ·	· · ·
· · ·	· · ·	· · ·	· · ·	1054.3(3)	3.4
· · ·	· · ·	· · ·	· · ·	1057(8)	· · ·
· · ·	· · ·	· · ·	· · ·	1063.0(7)	2−,5−
1067.4	4−	1067.424	4−	· · ·	· · ·
· · ·	· · ·	1068.992	5−	1068.5(3)	3,4
· · ·	· · ·	· · ·	· · ·	1074(5)	(5−)
· · ·	· · ·	· · ·	· · ·	1080.3(3)	5−,(2−)
1100.4	3−	1100.408	3−	1101.0(3)	· · ·
1104.6	4−	· · ·	· · ·	1104.2(16)	· · ·
1120.2	(3–6)	· · ·	· · ·	· · ·	· · ·
· · ·	· · ·	· · ·	· · ·	1129.7(16)	· · ·
1142.3	(0–4)	· · ·	· · ·	· · ·	· · ·

TABLE II. (*Continued*).

This work		(*n*,gamma)		Nuclear Data Sheets	
Energy (±0.1)	Adopted J^π	Energy [7] (±0.01)	J^π	Energy [8]	J^π
1163.9	(1–5)	· · ·	· · ·	1162(4)	· · ·
· · ·	· · ·	· · ·	· · ·	1168.6(16)	3,4
· · ·	· · ·	· · ·	· · ·	1182(5)	· · ·
1227.8	(1–5)	· · ·	· · ·	1225.3(16)	3,4
1237.4	(2–6)	· · ·	· · ·	1236.9(16)	3,4
1241.0	(4–8)	· · ·	· · ·	· · ·	· · ·
1274.5	(2–6)	· · ·	· · ·	1273(2)	(7)+
1277.7	(4–8)	· · ·	· · ·	· · ·	· · ·
· · ·	· · ·	· · ·	· · ·	1294(2)	· · ·
1301.4	(1–5)	· · ·	· · ·	· · ·	· · ·
· · ·	· · ·	· · ·	· · ·	1326(3)	· · ·
· · ·	· · ·	· · ·	· · ·	1349(5)	· · ·
1370.7	(2–6)	· · ·	· · ·	· · ·	· · ·
· · ·	· · ·	· · ·	· · ·	1395.0(14)	(5)−
1426.0	(2–6)	· · ·	· · ·	1426(9)	· · ·
· · ·	· · ·	· · ·	· · ·	1462.0(14)	8+
· · ·	· · ·	· · ·	· · ·	1510(2)	· · ·
· · ·	· · ·	· · ·	· · ·	1533(2)	(6)−
· · ·	· · ·	· · ·	· · ·	1569(5)	· · ·
· · ·	· · ·	· · ·	· · ·	1593(9)	· · ·
· · ·	· · ·	· · ·	· · ·	1617(5)	· · ·
· · ·	· · ·	· · ·	· · ·	1655(2)	(9)+
· · ·	· · ·	· · ·	· · ·	1679(1)	· · ·
· · ·	· · ·	· · ·	· · ·	1689(7)	· · ·
· · ·	· · ·	· · ·	· · ·	1730(7)	(7−)

els in many cases from this more detailed work. In those cases where we alone identify levels, we assume that the spins can be inferred by assuming that $\Delta J \leq 2\hbar$ for the resultant transitions. We have identified a specific level at 838.5 keV which decays both to the ground state and to the isomer. The 838.5 keV level can then serve as an equilibration path between the two levels, and through photoexcitation alone guarantee that the two levels are in equilibrium for temperatures $> 3\times10^8$ K. In addition to photoexcitation, the processes of Coulomb excitation, inelastic neutron scattering, and positron annihilation excitation will also contribute to the equilibration of the two levels and will reduce the temperature where the two levels achieve equilibration. Also, we would expect that the levels at 722.9 and 563.9 might serve as mediating levels and would significantly reduce the equilibration temperature. This equilibration of the ground state and isomer rules out the use of ^{176}Lu as an *s*-process chronometer. The extreme temperature sensitivity of the effective half-life of ^{176}Lu also complicates efforts to deduce the *s*-process temperature profile.

TABLE III. The decay strengths for the five transitions from the level at 838.5 keV. These strengths obtained by gating on any of the five transitions populating the level have been corrected for the detector efficiency, but have not been corrected for internal conversion. The errors shown in the third column are statistical (1σ) errors.

E_γ (keV)	I_γ (%)	(σ_{I_γ}) (%)
115.7	3.1	±0.5
181.2	4.9	±0.4
203.5	7.9	±0.5
274.6	13.9	±0.8
838.3	70.2	±2.9

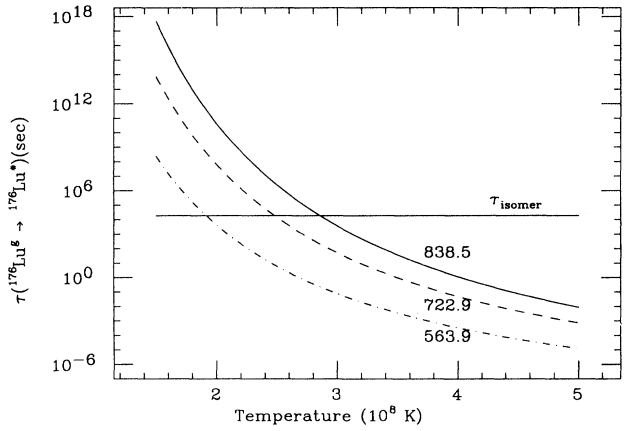

FIG. 12. The population time of the mediating level at 838.5 keV as a function of temperature for the ground state (solid curve). Assuming that the populating time is short (i.e., $\frac{1}{10}$) in comparison to the mean-life (horizontal solid line) of the isomer establishes the temperatures where the isomer and ground state will be in thermal equilibrium. Analogous curves for possible mediating levels at 722.9 (dashed) and 563.9 keV (dash-dotted) are also presented.

TABLE IV. Estimated effective β-decay half-lives for ^{176}Lu for a variety of temperatures between 0 and 5×10^8 K.

Temperature (10^8 K)	Ref. [18]	Ref. [19]	$t_{1/2}(^{176}\mathrm{Lu})$ (yr) This work
0	...	...	4.08×10^{10}
1	5.070×10^3	5.28×10^3	3.29×10^3
1.5	...	...	28.3
2	2.66	3.17	2.63
2.5	...	...	0.634
3	0.143	0.230	0.245
3.5	...	...	0.125
4	0.026	0.053	0.0750
4.5	...	...	0.0506
5	0.0082	0.019	0.0370

TABLE V. The various parameters needed to calculate Δ_{max} using Eq. (4).

$\lambda_{^{176}\mathrm{Lu}}=1.70\times10^{-11}$ yr^{-1}	Ref. [2]
$\langle N_s\sigma\rangle_{176}=8$ mb (Si$=10^6$)	Ref. [29]
$N_{^{176}\mathrm{Lu}}=0.001\,035$ (Si$=10^6$)	Ref. [30]
$\langle\sigma_{^{176}\mathrm{Lu}}\rangle=1537$ mb	Ref. [31]
$B=0.11\pm0.04$	Ref. [32]
(based on $\sigma_{\mathrm{tot}}=1203\pm10$ mb, $\sigma_{\mathrm{iso}}=1036\pm2$),	Ref. [31]

ACKNOWLEDGMENTS

We would like to express our appreciation to M. A. Deleplanque, R.M. Diamond, and F.S. Stephens for their assistance in operating HERA, to the crew and staff of the 88-Inch Cyclotron for the operation of the ECR source and cyclotron, and Dr. E. Browne, for his assistance with details in the analysis. This work was supported by the Director, Office of Energy Research, Office of High Energy and Nuclear Physics, Division of Nuclear Physics, of the U.S. Department of Energy under Contract NO. DE-AC03-76SF00098 and by the National Science Foundation's Science and Technology Center Research Program under Cooperative Agreement No. AST-8809616.

*Present address: Oliver Lodge Laboratory, University of Liverpool, Physics Department, BN 147 Liverpool, L69 3BX, United Kingdom.

[1] C. M. Lederer and V. S. Shirley, *Table of Isotopes,* 7th ed., (Wiley, New York, 1978).
[2] E. B. Norman, Phys. Rev. C **21**, 1109 (1980).
[3] J. Audouze, W. A. Fowler, and D. N. Schramm, Nature **238**, 8 (1972).
[4] M. Arnould, Astron. Astrophys. **22**, 311 (1973).
[5] E. B. Norman, T. Bertram, S. E. Kellogg, S. Gil, and P. Wong, Astrophys. J. **291**, 834 (1985).
[6] N. Klay, in *Proceedings of the 5th Workshop on Nuclear Astrophysics, Ringberg Castle, Tegernsee, F.R.G., 1989,* edited by W. Hillebrandt and E. Müller (1989) p. 12; private communication.
[7] N. Klay, Ph.D. thesis, Kernforschungzentrum Karlsruhe, Institue für Kernphysik (Von der mathematisch-naturmissenschaftlichen Gesamtfakultät der Ruprecht-Karls-Universität Heidelberg genehmigte Dissertation—Report KFK 4675, 1990); N. Klay *et al.*, Phys. Rev. C **44**, 2801 (1991).
[8] E. Browne, Nucl. Data Sheets **60**, 227 (1990).
[9] R. A. Dewberry, R. K. Sheline, R. G. Lanier, L. G. Mann, and G. L. Struble, Phys. Rev. C **24**, 1628 (1981).
[10] M. M. Minor, R. K. Sheline, E. B. Shera, and E. T. Jurney, Phys. Rev. **187**, 1516 (1969).
[11] G. L. Struble and R. K. Sheline, Yad. Fiz. **5**, 1205 (1966) [Sov. J. Nucl. Phys. **5**, 862 (1967)].
[12] J. Gerl, K. Ronge, K. Venkata Ramaniah, Th.W. Elze, A. Hanser, and L. D. Tolsma, Z. Phys. A **310**, 349 (1983).
[13] O. A. Wasson and R. E. Chrien, Phys. Rev. C **2**, 675 (1970).
[14] R. W. Hoff, R. F. Casten, M. Bergoffen, and D. D. Warner, Nucl. Phys. **A437**, 285 (1985).
[15] A. K. Jain, J. Kvasil, R. K. Sheline, and R. W. Hoff, Phys. Rev. C **40**, 432 (1989).
[16] M. K. Balodis, J. J. Tambergs, K. J. Alksnis, P. T. Prokofjev, W. G. Vonach, H. K. Vonach, H. R. Koch, U. Gruber, B.P.K. Maier, and O.W.B. Schult, Nucl. Phys. **A194**, 305 (1972).
[17] W. A. Fowler, G. R. Caughlan, and B. A. Zimmerman, Annu. Rev. Astron. Astrophys. **5**, 525 (1967).
[18] K. Cosner and J. W. Truran, Astrophys. Space Sci. **78**, 85 (1981).
[19] K. Takahashi and K. Yokoi, Data Nucl. Data Tables **36**, 375 (1987).
[20] D. N. Schramm and G. J. Wasserburg, Astrophys. J. **162**, 57 (1970).
[21] B. J. Allen, G. C. Lowenthal, J. W. Boldeman, and J. R. De Laeter, Proceedings of the 5th International Conference on Geochronology, Cosmochronology, and Isotope Geology, 1982, Nikko Park, Japan (1982).
[22] B. J. Allen, G. C. Lowenthal, and J. R. De Laeter, J. Phys. G **7**, 1271 (1981).
[23] H. Beer and F. Käppeler, Phys. Rev. C **21**, 534 (1980).
[24] R. L. Macklin and J. H. Gibbons, Phys. Rev. **159**, 1007 (1967).
[25] J. R. De Laeter, B. J. Allen, G. C. Lowenthal, and J. W. Boldeman, J. Astrophys. Astron. **9**, 7 (1988).
[26] H. Beer, F. Käppeler, K. Wishak, and R. A. Ward, Astrophys. J. Suppl. **46**, 295 (1981).
[27] H. Beer, Astrophys. J. **262**, 739 (1982).
[28] F. Käppeler, H. Beer, and K. Wisshak, Rep. Prog. Phys. **52**, 945 (1989).
[29] E. Anders, N. Grevesse, Geochim Cosmochim. Acta **93**, 197 (1989).
[30] Z. Y. Bao and F. Käppeler, Data Nucl. Tables **36**, 411 (1987).
[31] W. R. Zhao and F. Käppeler, Fifth IAP Astrophysics Meetings on Astrophysical Ages and Dating Methods, Paris, 1989 (unpublished); Phys. Rev. C **44**, 506 (1991).